ZnS Nano-architectures: Photocatalysis, Deactivation and Regeneration

--Supplementary Material

Dagui Chen, Feng Huang, Guoqiang Ren, Dongsong Li, Meng Zheng, Yongjing Wang and Zhang Lin**

Key Laboratory of Optoelectronic Materials Chemistry and Physics, Fujian Institute of Research on the Structure of Matter, Chinese Academy of Sciences, Fuzhou, Fujian, 350002, China

*Corresponding author: fhuang@fjirsm.ac.cn, zlin@fjirsm.ac.cn

Surface acidification treatment enhancing the photocatalytic activity of ZnS microspheres.

After the neutralization of the excess OH^- on the surface, ZnS nano-architectures exhibit remarkable increase in photocatalytic activity while still maintaining the initial size and morphology (Fig. S1).

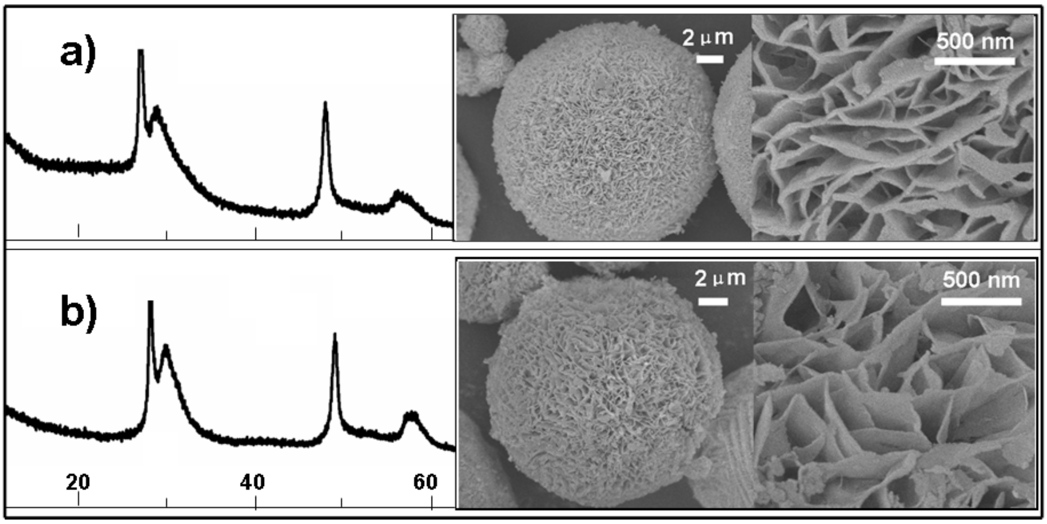

Figure S1. The XRD pattern (left) and SEM image (right) of ZnS microspheres a) before b) after the neutralization of the excess surface OH^- by adding dilute acetic acid solution (1.0×10^{-2} M).

Control experiments for photodegradation of eosin B.

The control experiments show that there is no obvious photocatalytic activity of both ZnS microsphere and Degussa P25 titania in the absence of UV light. Under the irradiation of UV light, the photocatalytic activity of the ZnS microsphere is close to that of Degussa P25 titania (Fig S2).

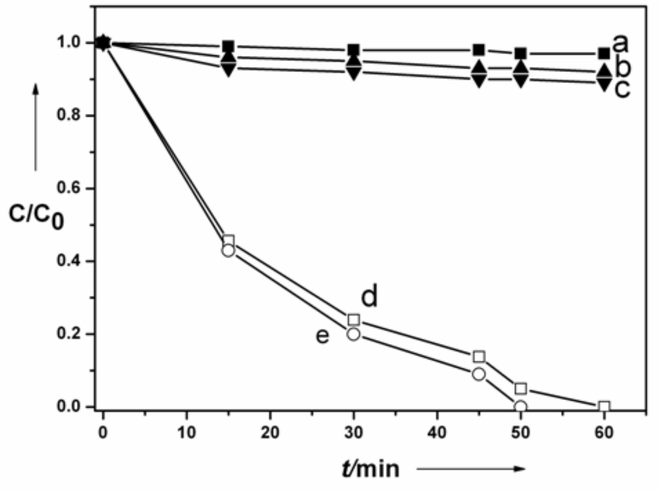

Figure S2. Photodegradation of eosin B (5.0 ×10^{-5} M, 30 mL) with 10 mg different kinds of catalyst: a) in the dark with Degussa P25 titania; b) in the UV light only; c) in the dark with ZnS microspheres; d) in the UV light with ZnS microspheres; e) in the UV light with Degussa P25 titania.

Brunauer–Emmett–Teller (BET) surface area measurements of ZnS at different states.

It shows that after six photocatalytic cycles, the BET surface area of the ZnS microspheres decrease from 124.7 m^2g^{-1} to 67.2 m^2g^{-1}. After recovery treatment in its thermodynamic condition, the BET surface area of the ZnS photocatalyst is around 120 m^2g^{-1}.

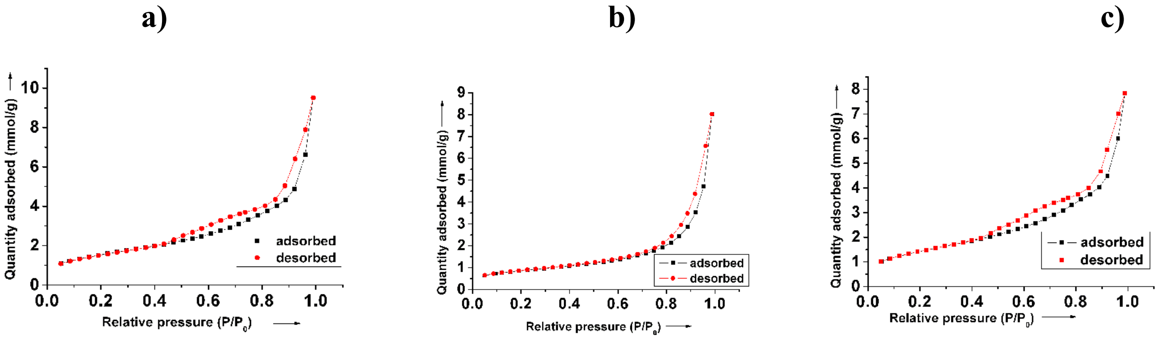

Figure S3. Nitrogen adsorption and desorption isotherm of a) initial ZnS microspheres, b) the deactivated ZnS microspheres after six photocatalytic cycles and c) the recovered ZnS microspheres.

Analysis of the recovery mechanism of ZnS microspheres.

The formation of ZnS solid microspheres is a growth based on the original ZnS microsphere interwoven by nanosheets. During this process, a part of nanosheets dissolved, and then re-precipitated on the nanosheets. The thickness of the nanosheets increased and at last the microsphere solidified.

As to the recovery of ZnS microsphere, it could not simply be regard as the reverse process of the formation process. The solution changed into 14M NaOH that saturated with ZnS. In this solution, the solubility of ZnS increase greatly, moreover, it is a negative interfacial free energy environment for ZnS[3]. The formation of nanosheets interwoven microsphere is a re-necleation and regrowth process. As shown in the following figure, the ZnS dissolved from solid microspheres and formed new crystal nucleus in the solution. Based on this new core, microsphere interwoven with nanosheets increasely grew. in such circumstance, the growth speed is high, and the finally product is dominated by ZnS microsphere interwoven by nanosheets.

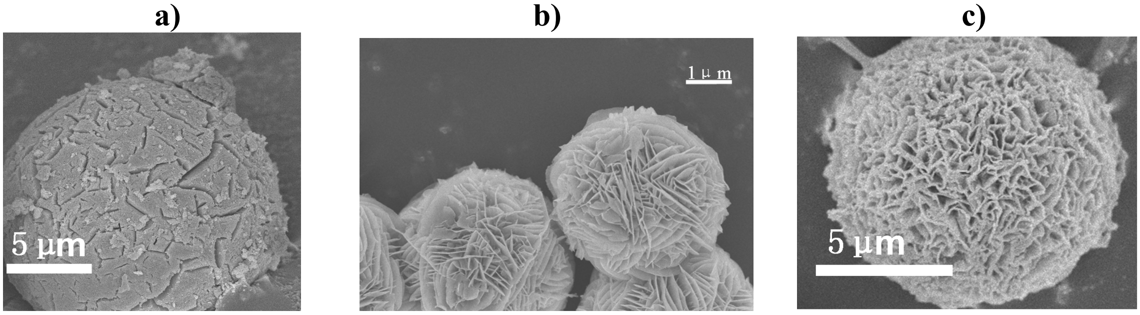

Figure S4 a)The deactivated ZnS solid microsphere; b) After in 14M NaOH solution saturated with ZnS for 12 hour, ZnS intermediate states were observed. The structure of the material was small sized ZnS microsphere that interwoven with nanosheets c)After in 14M NaOH solution saturated with ZnS for 24 hour, the ZnS microspheres grew quickly that the size of the porous structured ZnS microsphere increased apparently.

The thermodynamically stable nanophases of ZnS and CdS.

According the second law of thermodynamics, the final reaction state represents the chemical equilibrium and the minimization of the Gibbs free energy of the whole system. Based on this rule, we have proved the thermodynamically stable nanophase of ZnS in 14 M NaOH is ZnS microsphere composed by interwoven nanosheets, and the thermodynamically stable nanophase of CdS in 4M KOH-*tert*-butyl alcohol solution is CdS nanosheet.

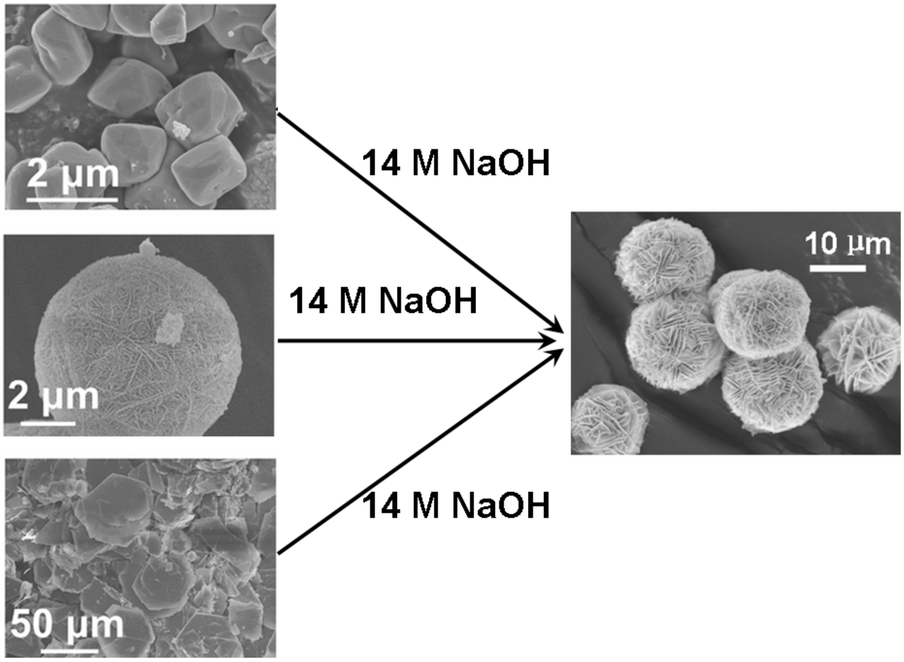

Figure S5. In 14 M NaOH, ZnS precursors at different sizes and morphologies transform into the final thermodynamically stable states (ZnS microspheres composed by interwoven nanosheets) spontaneously.

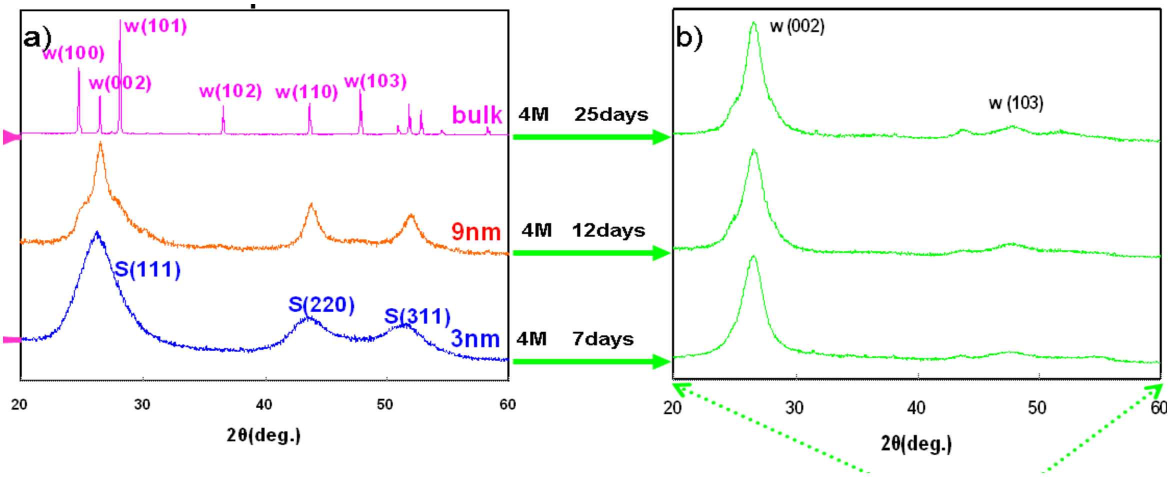

Figure S6. XRD data showing the transformation relations among CdS initial samples and resulting CdS nanosheet samples. a) CdS initial sample, 3 nm CdS (blue curves, cubic sphalerite phase), bulk CdS (pink curves, hexagonal wurtzite phase), and 9nm CdS (nacarat curves, mixture of sphalerite phase and wurtzite phase). b) CdS nano-sheets (green curves) from various CdS initial samples under hydrothermal condition at 180 °C in the 4M KOH- *tert*-butyl alcohol solution.

The thermodynamic equilibrium reaction of ZnS nano-material in 14M NaOH solutions.

$$\mathrm{ZnS(solid\ sphere)+4NaOH} \rightarrow \mathrm{Na_2ZnO_2(aq)+Na_2S(aq)+2H_2O} \quad (1)$$

$$Na_2ZnO_2(aq)+Na_2S(aq)+2H_2O \rightarrow ZnS(\text{solid microsphere})+4NaOH \quad (2)$$

The reason why ZnS particles exhibited the higher photocatalytic activity

Except for the high BET surface area (124 m^2g^{-1}) and aggregation-free characters, the higher photocatalytic activity of the synthetic ZnS photocatalysts could also originate from the intrinsic properties of the materials listed as follows:

1. **The polarization crystal structure of ZnS materials:** The produced ZnS microspheres are composed of 20-30 nm interwoven nanosheets, with wurtzite ZnS (0001) face as exposure crystal face. As shown in figure S7, owing to the positive and negative ionic charges on the zinc- and sulfur-terminated ± (0001) surfaces of ZnS, respectively, a spontaneous polarization is induced across the ZnS nanosheets from Zn-terminated plane to S-terminated plane. The polarization electric field in the nanosheets would facilitate the separation of light-induced electrons and holes, and accelerate them to diffuse to the surfaces of the materials. This phenomenon was also observed in ZnO single crystal, which has the similar crystal structure and polarization electric field (*Wang YH, Huang F et al, Chem. Commun., 2009, 44, 6783-6785*).

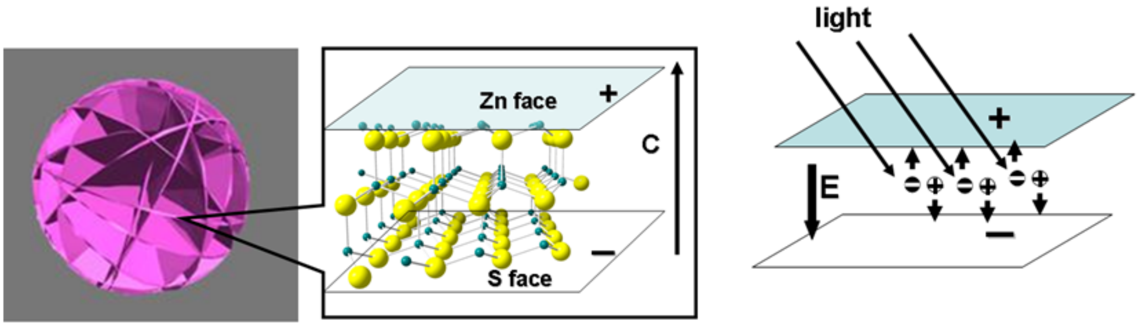

Figure S7. The polarization electric field in the ZnS nanosheets would facilitate to separate the light-induced electrons and holes, and accelerate them to diffuse to the surfaces of the materials

2. **The higher photocarrier generation efficiency of ZnS materials:** It is well known that TiO_2 materials is an indirect band-gap semiconductor, thus the generation efficiency of photocarrier is low (figure S8a). However, ZnS is a direct band-gap semiconductor, as shown in figure S8B, the generation efficiency of photocarrier is higher.

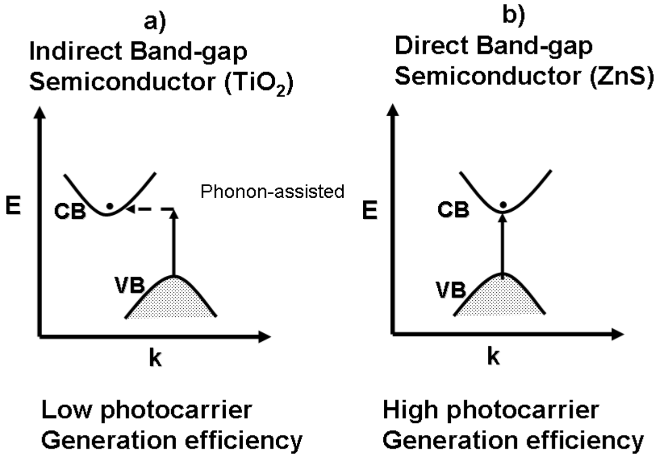

Figure S8. a) For indirect band-gap semiconductor, the process of the electron transition from the VB(Valence Band) to CB(Conductive Band) needs the assistance of phonon, which results in low transition probability. **b)** For direct band-gap semiconductor, the electron transition process is not involved with phonon, thus the transition probability is high.

In summary, theoretically, the photocatalytic activity of ZnS material should be higher than that of P25 due to the polarization crystal structure and higher photocarrier generation efficiency.

However, in many reports, ZnS material have not shown higher photocatalytic activity than P25. We believe that the reason probably lies in the much lower lattice energy of ZnS than TiO2, which is easier to induce internal lattice defects and surface defects of ZnS (As we known, such defects are photocarrier trap during the transfer process of photocarrier). In the other study, we find the catalytic activity of ZnS nano-photocatalyst could be greatly enhanced once the lattice defects and surface defects were “popped out” via annealing treatment.

1 G. Q. Ren, Z. Lin, B. Gilbert, J. Zhang, F. Huang, J. K. Liang, *Chem. Mater.* 2008, **20**, 2438-2443.

2 D. S. Li, Z. Lin, G. Q. Ren, J. Zhang, J. S. Zheng, F. Huang, *Cryst. Grow. & Des.* 2008, **8**, 2324-2328.

3 Z. Lin, B. Gilbert, Q. L. Liu, G. Q. Ren, F. Huang, *J. Am. Chem.* Soc. 2006, **128**, 6126-6131.